Nanoscale

Accepted Manuscript

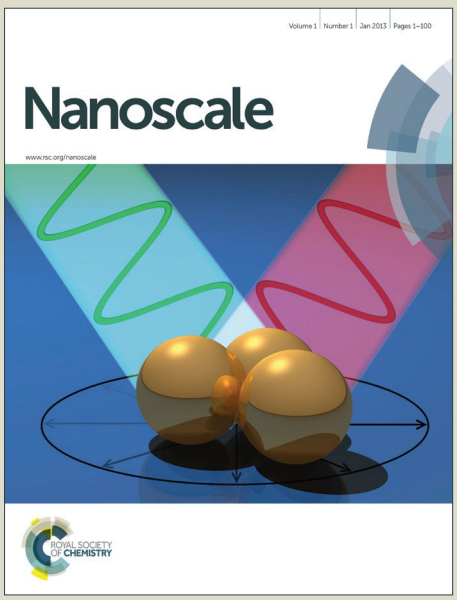

ROYAL SOCIETY OF CHEMISTRY

www.rsc.org/nanoscale

Three-dimensional nitrogen-doped graphene as an ultrasensitive electrochemical sensor for the detection of dopamine

Xiaomiao Feng, *[1a] Yu Zhang, [1a] Jinhua Zhou, [1] Yi Li, [1] Shufen Chen, [1] Lei Zhang, [1] Yanwen Ma, *[1] Lianhui Wang,[1] and Xiaohong Yan [2]

1. Key Laboratory for Organic Electronics and Information Displays & Institute of Advanced Materials, National Jiangsu Syngerstic Innovation Center for Advanced Materials (SICAM). 2. College of Electronic Science and Engineering, Nanjing University of Posts & Telecommunications, 9 Wenyuan Road, Nanjing 210023, China

**Corresponding author.*

E-mail: iamxmfeng@njupt.edu.cn; iamywma@njupt.edu.cn

[a] *These authors contributed to this work equally.*

Abstract

Three-dimensional nitrogen-doped graphene (3D N-doped graphene) was prepared through the chemical vapor deposition (CVD) by using porous nickel foam as a substrate. As a model, a dopmine biosensor was constructed based on the 3D N-doped graphene porous foam. Electrochemical experiments exhibited that this biosensor had remarkable detective ability with a wide linear detection range from 3×10^{-6} M to 1×10^{-4} M and a low detection limit of 1 nM. Moreover, the fabricated biosensor also showed excellent anti-interference ability, reproducibility, and stability.

Introduction

Graphene, a two-dimensional structure material composed of carbon atoms, has attracted enormous attentions due to its extraordinary electrical, optical, structural, and mechanical properties.[1-5] However, the chemically derived two-dimensional graphene-based composites usually suffer from poor conductivity as a result of low quality or high junction contact resistance of the graphene sheets. [6,7] Graphene foam, a kind of three-dimensional (3D) structure graphene-based material, has a wide range application in the field of electronic devices, supercapacitors, and sensors due to its remarkable conductivity, high specific surface area, and good biocompatibility.[8-11] The graphene foams fabricated by chemical vapor deposition (CVD) method display highly conductive defect-free graphene layers without the formation of junction resistance.[6, 12] The highly electrical conductive network structure and the large specific area of the 3D graphene foam provide carriers for the electron transportation processes and are suitable for biosensing.[13-15]

The electronic properties, surface structure, and other intrinsic properties of the carbon materials can be effectively tuned and enhanced by the chemical doping with hetero-atoms.[16-18] The presence of the dopant atoms lead to the local chemical changes to the elemental composition of the host material, which can improve the thermal or conductivities and enrich the charge-carrier densities.[19] Among numerous dopants, nitrogen is widely used to be doped with the graphene-based materials. The N doped carbon nanotubes/graphene (NCNTs/G) has been used in the application of oxygen reduction reaction in alkaline electrolyte, which showed higher activity and selectivity compared with undoped CNTs/G composites.[20] Zhu et al. has developed a

new electrochemical immunosensor based on the effective assembly of gold nanoparticles and nitrogen-doped graphene sheets for ultrasensitive detection of matrix metalloproteinase-2 with a low detection limit of 0.11 pg mL^{-1}.[21]

Dopamine (DA) distributed in mammalian brain has been widely and deeply studied since its discovery in 1950s.[22] As one of the most significant neurotransmitters in the mammalian central nervous system, DA is a key maker for the treatment of schizophrenia and Parkinson's disease.[23, 24] Therefore, the rapid and accurate measurement to detect the trace amount of DA is of extreme importance to the clinical diagnosis and prevention of the diseases caused by the abnormal control of DA concentration in human bodies. As DA can be easily oxidized electrochemically, the electrochemical method is widely used to detect it.[25, 26] However, the interferences of AA and UA, which mostly coexist with DA and have the similar oxidation potential to DA, can lead to an overlapping voltammetric response in the electrochemical method.[27, 28] Therefore, a sensor with improved high selectivity and sensitivity to the detection of DA is quite essential.

In the present work, 3D N-doped graphene foam was prepared by the chemical vapor deposition (CVD) using the nickel foam as a substrate. Combining the advantages of well-defined 3D structure and doped nitrogen atoms, the obtained free-standing 3D N-doped graphene exhibited high electrical conductivity, satisfactory biocompatibility and electroactivity, and was developed as electrode materials for the electrochemical detection of DA. The resulting sensor showed excellent electrochemical activity, selectivity, sensitivity, and stability to the detection of DA in neutral solutions.

Experimental Section

Preparation of 3D N-doped graphene electrodes

The 3D N-doped graphene was synthesized by chemical vapor deposition (CVD) method. Typically, a piece of nickel foam (2 cm × 2 cm, thickness 1.0 mm) was acted as the growth template and put into a quartz tube under H_2 (20 sccm) and Ar (200 sccm). Ethylenediamine (0.25 mL) was the precursor and the reaction temperature was raised from room temperature to 900 °C at a heating rate of 10 °C min^{-1}. The reaction was allowed to proceed for 30 min. Then, after cooling down to room temperature, the nickel foam was removed to obtain the final product as the follow procedure.[6, 8] The 3D N-dpoed graphene/Ni foam was drop-coated with a poly (methyl methacrylate) (PMMA) solution, and then dried for 10 min at 150 °C. Thus, a thin PMMA film that could prevent the destruction of the graphene structure upon the remove of the nickel template was formed on the N-doped graphene surface. Then, nickel was removed by immersing the sample in HCl (3 M) solution at 80 °C for 5 h. Finally, the free-standing 3D N-doped graphene was obtained by dissolving the PMMA protective layer in hot acetone. Then, after washed by the deionized water, the freestanding 3D N-doped graphene was fabricated as an electrochemical electrode.

Characterization

The products were characterized by scanning electron microscopy (SEM, S-4800),

X-ray photoelectron spectroscopy (XPS, PHI5000 VersaProbe) and Raman spectroscopy (Renishaw inVia Raman Microscope with an argon-ion laser at an excitation wavelength of 514 nm). The static water contact angles were measured with a contact angle meter (Rame-Hart-100, USA) using droplets of deionized water at room temperature. Electrochemical experiments were conducted with a CHI660C workstation (Shanghai Chenhua, Shanghai) in a three-electrode system. All electrochemical experiments were performed in a cell containing 6.0 mL of phosphate buffer solution (PBS, 0.1 M) at room temperature, using a coiled platinum wire as the auxiliary electrode, a saturated calomel electrode (SCE) as the reference electrode, and the different materials-fabricated electrode as the working electrode.

Results and Discussion

The morphology of the CVD-grown free-standing 3D nitrogen-doped graphene foam is characterized by scanning electron microscopy (SEM). A well-defined foam-like porous structure of the nitrogen-doped graphene is shown in Fig. 1a. The pore diameter ranges from about 200 to 600 μm. Fig 1b is the image of the gap on the edge of the 3D N-doped graphene sketeton. The gap was caused on purpose in the SEM sample preparation process to prove the hollow skeleton structure and the successful removal of the Ni foam substrate. Fig. 1c exhibits the image of the surface of graphene skeleton and Fig 1d is a higher magnification display. As a result of the conformal CVD grown, the surface of the thin graphene skeleton is smooth as the same surface topological features of the Ni substrate.[29] The obvious ripples and wrinkles on the graphene surface, which are the typical features of the CVD-grown graphene, were generated from the different thermal expansion during the grown process.[30]

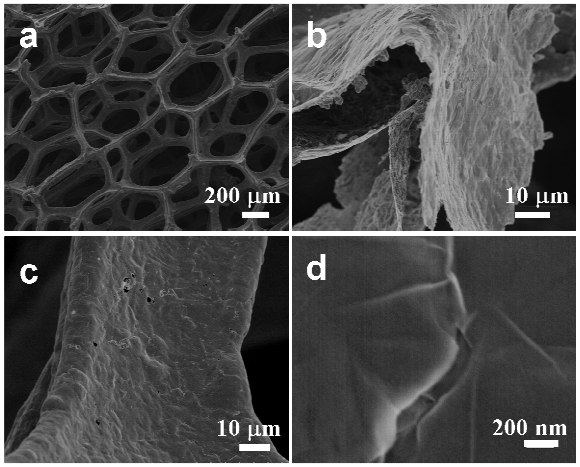

Fig. 1 SEM images of (a) free-standing 3D N-doped graphene sketeton, (b) 3D N-doped graphene skeleton gap, (c) the surface of 3D N-doped graphene skeleton, and (d) the high magnification display of the 3D N-doped graphene surface.

The Raman spectra of 3D-graphene and 3D N-doped graphene foam obtained at different positions are demonstrated in Fig. 2. Three salient characteristic peaks at around 1357, 1580, and 2700 cm^{-1} appears in the Raman spectra, corresponding to the

D, G and 2D bands of graphene, respectively.[31] Compared with the spectrum of 3D-graphene, the D-band peak at ~ 1350 cm^{-1} is obtained in the N-doped graphene sample and the intensity ratio of the D band to the G band (I_D/I_G) is 0.49. It indicates that the doped nitrogen atoms lead to the disorder-induced band and the indicative of defects in the graphene structure.[32] And the G-band, peak at ~1580 cm^{-1}, is attributed to $C(sp^2)$-$C(sp^2)$ band stretching vibrations.[33, 34] The presence of the 2D peak indicates that the multi-layer graphene exists in the product.[29]

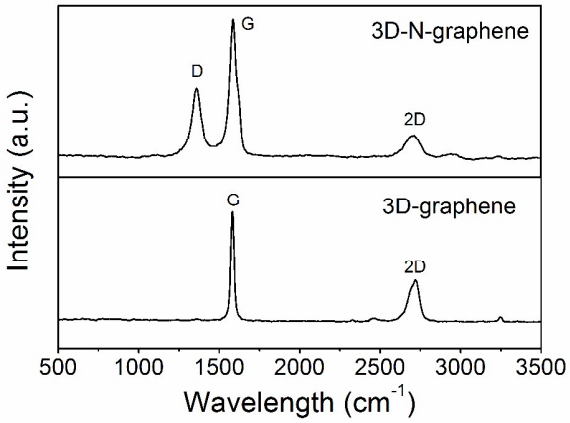

Fig. 2 Raman spectra of 3D N-doped graphene and 3D-graphene.

The content and state of nitrogen element in 3D N-doped graphene were analyzed by X-ray photoelectron spectroscopy (XPS). Fig.3 displays the survey scan of 3D-N-graphene, 3D-graphene, and N1s narrow scan XPS spectra of 3D N-doped Graphene. As can be seen in Fig .3a, a predominant narrow C1s peak at ~285 eV is obtained in both of the 3D N-doped graphene and the 3D graphene, while the N1s peak at ~400 eV was presented only in the N-doped 3D graphene. The corresponding element contents in the 3D-N-graphene are 97.29% and 2.71% for C 1s and N 1s, respectively. The content of Ni was measured to be zero indicating that the remove of Ni substrate was successful by the acid treatment. The high resolution XPS N1s spectrum shown in Fig.3b revealed the presence of five component of nitrogen atoms within the graphene structure, including pyridinic N (398.3 eV), pyrrolic N (400.4 eV), graphitic N (401.3 eV), N-oxide (403.3 eV), and N_2 (405.5 eV).[20, 35, 36]

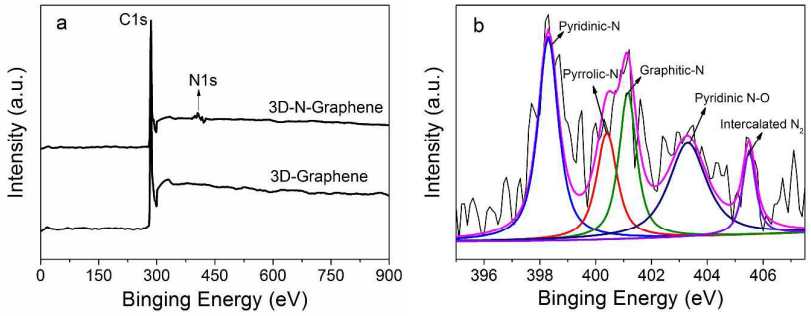

Fig. 3 XPS spectra of (a) survey scan of 3D N-doped graphene and 3D-graphene, and (b) N1s narrow scan of 3D N-doped graphene.

Electrochemical activity of the as-prepared 3D N-doped gragpene is detected by cyclic voltammetric (CV) experiments. Fig. 4 represents the CV behaviors of the different materials in 0.1 M PBS 7.0 solutions with or without the presence of DA. No redox peak was obtained of the 3D N-doped graphene fabricated electrode in the blank PBS without DA (Fig. 4e). Nevertheless, after the addition of 1 mM DA, an obvious pair of redox peak appeared (Fig. 4d). Among several CV curves of Fig. 4a-d which corresponding to different graphene-based material fabricated electrode in 1mM DA, including (a) 2D-Graphene, (b) 3D-Graphene, (c) 2D-N-Graphene, and (d) 3D-N-Graphene, Fig. 4d showed the lowest potential and the highest current value suggesting that 3D-N-Graphene has the best eletrocatalytic activity towards the detection of DA. These results implied that the 3D structure and the doped-N atom of 3D-N-Graphene could lead to the enhancement of the electron transfer rate and improvement of the electrocatalytic activity.

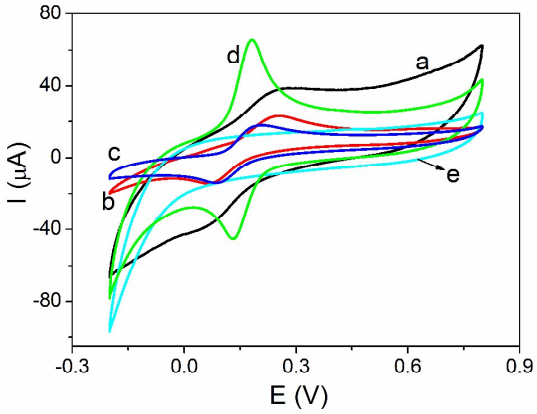

Fig. 4 Cyclic voltammograms of different graphene-based electrodes in 0.1 M PBS (pH = 7.0) containing 1 mM DA at the scan rate of 100 mV/s: (a) 2D-Graphene, (b) 3D-Graphene, (c) 2D-N-Graphene, (d) 3D-N-Graphene with 1 mM DA, and (e) 3D-N-Graphene without DA.

The effect of the potential scan rate (v) on the peak current for the 3D N-doped graphene fabricated biosensor with the presence of 1 mM DA in the range of 50-500 mV/s is shown in Fig. 5. The anodic peak potential shifts to a more positive direction and the cathodic peak potential shifts toward a more negative direction with the increase of the scan rates. And peak currents increase linearly with the increase of the square root of the scan rate ($v^{1/2}$), indicating a diffusion controlled process.[37, 38]

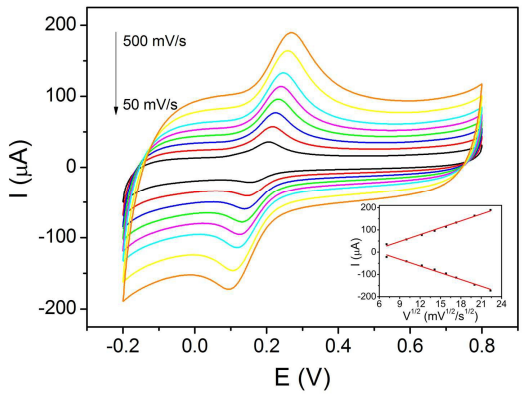

Fig. 5 3D N-doped graphene electrodes in 0.1 M PBS (pH = 7.0) with 1mM DA at different scan rates: from inside to outside 50, 100, 150, 200, 250, 300, 400, and 500 mV/s. Insets show calibration plots between oxidation peak currents and the square root of the scan rate.

The anti-interference property of the proposed biosensor was tested by selective detection with glucose (GC), ascorbic acid (AA), and uric acid (UA) that usually coexist with DA. As it is shown in Fig. 6, the current response of 1.0 mM DA, 1.0 mM GC, 1.0 mM AA, and 1.0 mM UA has been studied through differential pulse voltammetric (DPV) experiments carried out in neutral electrolyte. An obvious oxidation peak appeared at around 0.13V after 1.0 mM DA was added while there was hardly any incremental of the current upon the addition of inferences suggesting that DA can be detected in the presence of GC, AA, and UA, showing the selectivity of the biosensor is very high. The possible reason for selective detection of DA may be the strong π-π interactions between the graphene basal plane and the phenyl ring of DA molecules, which makes it more possible for DA to absorb on the surface of the graphene foam leading to an enhanced and specific voltammetric response of DA.[39, 40, 41]

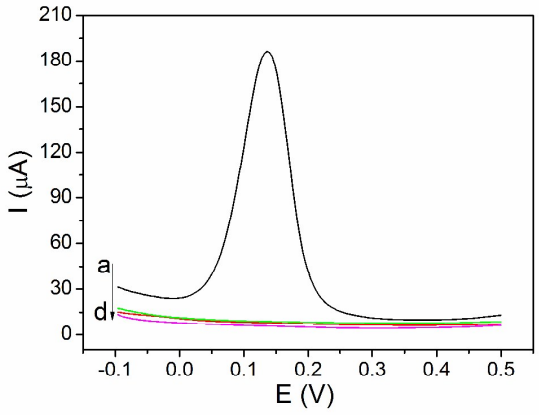

Fig. 6 Differential pulse voltammograms of the 3D N-doped graphene fabricated electrode in 0.1 M PBS (pH = 7.0) with 1 mM (a) DA, (b) GC, (c) AA, and (d) UA, respectively.

The detection linear range and the detection limit of the biosensor were obtained by the DPV measurements using the 3D N-doped graphene eletrode in pH 7.0 PBS upon the successive addition of different concentration of DA solutions. To make sure that the added DA was fully mixed, the electrolyte was stirred for about 1 min. CV was carried out until the peak current was stable and changeless and then the DPV was performed immediately. The peak at around 0.13 V appeared with the addition of DA. And the peak current gradually increased and was proportional to the DA concentrations with a wide linear range from 3×10^{-6} M to 1×10^{-4} M with the correlation coefficient of 0.9962. Furthermore, the biosensor exihibits remarkalbe sensitivity of 9.87 mA mM^{-1} cm^{-2} and a low detection limit of 1 nM at the signal-to-noise of 3. Table 1 shows the comparison of different graphene-based electrodes towards the electrochemical detection of DA. From the table, we can see that the 3D N-doped graphene foam electrode shows wider detection range, lower detection limit, and better sensitivity and selectivity in neutral environment than that of the other graphene-based electrodes. This may be due to the high conductivity, the perfect three dimensional structure of the 3D N-doped graphene foam, and good hydrophilicity and biocompatibility which is essential to the enhancement of electroactivity to the detection of DA.[30] The contact angle measurements have been taken to quantitatively evaluate the hydrophilicity and biocompatibility of the mearsured materials. Normally, the contact angle of pure graphene is above 90º.[45] The contact angle of 3D N-doped graphene foam is 70.9º reflecting its good hydrophilicity and biocompatibility which is caused by the existence the doped N atoms.

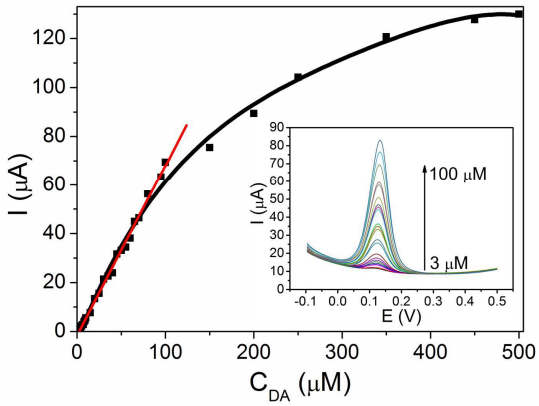

Fig. 7 Relationship between peak currents and the DA concentration. Insets are the DPV responses of different DA concentrations from 3 μM to 100 μM.

Electrodes	Detection range (μM)	Detection limit (nM)	Sensitivity (mA mM^{-1} cm^{-2})	Selectivity	pH	Ref.
EDTA-reduced graphene /Nafion /GC	0.2-25	10	—	AA	7.2	42

Graphene oxide nanoribbons /GCE	0.15-12.15	80	2.39	AA, UA	7.0	43
3D Graphene	Up to 25	25	0.62	UA	7.2	39
rGO/TiO_2{001}/GCE	2-60	6000	8.80	AA	6.5	44
3D N-doped Graphene (This work)	3-100	1	9.87	AA, UA, GC	7.0	—

Table 1. Comparison of different graphene-based electrodes towards the electrochemical detection of DA.

The reproducibility and stability of the 3D N-doped graphene electrode were further studied. When the electrode was successively scanned for 100 cycles, no obvious change in the peak current could be observed. The relative standard deviation (RSD) was 3.0% for six successive determinations. The fabrication of six electrodes made independently showed an acceptable reproducibility with a RSD of 3.9% for the current determined in the presence of 1 mM DA. The long-term stability of the electrode was investigated over a 10 day period. When the fabricated electrodes were stored in pH 7.0 PBS or dried in air at 4 °C, and measured periodically, no obvious change was found. These results showed the excellent reproducibility and stability of the 3D N-doped graphene-based DA biosensor, which might be attributed to the excellent conductivity and good biocompatibility of 3D N-doped graphene.

Conclusions

The successful synthesis of three-dimensional nitrogen-doped graphene (3D N-doped graphene) was achieved through the chemical vapor deposition (CVD) by using porous nickel foam as a substrate. The obtained free-standing 3D N-doped graphene was developed as an electrode material for the electrochemical detection of dopamine (DA). The fabricated biosensor showed high electrocatalytic activity to DA compared with other graphene-based electrode material. Furthermore, the biosensor exhibited excellent anti-interference ability, reproducibility, stability, and displayed a wide linear detection range from 3×10^{-6} M to 1×10^{-4} M with a low detection limit of 1 nM.

Acknowledgment

We sincerely express our thanks to the '973' (2012CB933301) and '863' projects (2011AA050526), the National Natural Science Foundation of China (Nos. 20905038, 20903057, 61205195, and 61274065), and the Natural Science Foundation of Jiangsu (BK20141424 and BK2011750), and the Priority Academic Program Development of Jiangsu Higher Education Institutions (PAPD), and the Ministry of Education of China (IRT1148).

References

1. X. Li, S. Zhu, B. Xu, K. Ma, J. Zhang, B. Yang and W. Tian, *Nanoscale*, 2013, **5**, 7776.
2. L. Li, A.-R. O. Raji and J. M. Tour, *Adv. Mater.*, 2013, **25**, 6298.
3. M. Sadhukhan, T. Bhowmik, M. K. Kundu and S. Barman, *RSC Adv.*, 2014, **4**,

4998.
4. M. Zhou, Y. Zhai and S. Dong, *Anal. Chem.,* 2009, **81**, 5603.
5. M. Zhou and S. Dong, *Acc. Chem. Res.*, 2011, **44**, 1232.
6. Z. Chen, W. Ren, L. Gao, B. Liu, S. Pei and H.-M. Cheng, *Nat. Mater.* , 2011, **10**, 424.
7. T. Zhai, F. Wang, M. Yu, S. Xie, C. Liang, C. Li, F. Xiao, R. Tang, Q. Wu, X. Lu and Y. Tong, *Nanoscale*, 2013, **5**, 6790.
8. Y. Xue, D. Yu, L. Dai, R. Wang, D. Li, A. Roy, F. Lu, H. Chen, Y. Liu and J. Qu, *Phys. Chem. Chem. Phys.* , 2013, **15**, 12220.
9. H. Huang, Y. Tang, L. Xu, S. Tang and Y. Du, *ACS Appl. Mat. Interfaces*, 2014, **6**, 10248.
10. Y. Ma, M. Zhao, B. Cai, W. Wang, Z. Ye and J. Huang, *Biosens. Bioelectron.*, 2014, **59**, 384.
11. B. Zhan, C. Liu, H. Chen, H. Shi, L. Wang, P. Chen, W. Huang and X. Dong, *Nanoscale*, 2014, **6**, 7424.
12. H. Y. Yue, S. Huang, J. Chang, C. Heo, F. Yao, S. Adhikari, F. Gunes, L. C. Liu, T. H. Lee, E. S. Oh, B. Li, J. J. Zhang, H. Ta Quang, L. Nguyen Van and Y. H. Lee, *ACS Nano*, 2014, **8**, 1639.
13. Y. Yang, C. Tian, J. Wang, L. Sun, K. Shi, W. Zhou and H. Fu, *Nanoscale*, 2014, **6**, 7369.
14. Y. J. Yun, W. G. Hong, N.-J. Choi, H. J. Park, S. E. Moon, B. H. Kim, K.-B. Song, Y. Jun and H.-K. Lee, *Nanoscale*, 2014, **6**, 6511.
15. B. Zhao, Z. Liu, W. Fu and H. Yang, *Electrochem. Commun.* , 2013, **27**, 1.
16. M. Lv, T. Mei, C. a. Zhang and X. Wang, *RSC Adv.*, 2014, **4**, 9261.
17. D. Jiang, Q. Liu, K. Wang, J. Qian, X. Dong, Z. Yang, X. Du and B. Qiu, *Biosens. Bioelectron.*, 2014, **54**, 273.
18. X. Xue, Q. Wei, D. Wu, H. Li, Y. Zhang, R. Feng and B. Du, *Electrochim. Acta*, 2014, **116**, 366.
19. P. Kannan, T. Maiyalagan, N. G. Sahoo and M. Opallo, *J. Mater. Chem. B*, 2013, **1**, 4655
20. Y. Ma, L. Sun, W. Huang, L. Zhang, J. Zhao, Q. Fan and W. Huang, *J. Phys. Chem. C*, 2011, **115**, 24592.
21. G. Yang, L. Li, R. K. Rana and J.-J. Zhu, *Carbon*, 2013, **61**, 357.
22. S. J. Park, H. S. Song, O. S. Kwon, J. H. Chung, S. H. Lee, J. H. An, S. R. Ahn, J. E. Lee, H. Yoon, T. H. Park and J. Jang, *Sci. Rep.*, 2014, **4**, 4342.
23. M.-C. Chuang, H.-Y. Lai, J.-a. Annie Ho and Y.-Y. Chen, *Biosens. Bioelectron.* , 2013, **41**, 602.
24. W. Wang, G. Xu, X. T. Cui, G. Sheng and X. Luo, *Biosens. Bioelectron.* , 2014, **58**, 153.
25. L. Liu, J. Du, S. Li, B. Yuan, H. Han, M. Jing and N. Xia, *Biosens. Bioelectron.* , 2013, **41**, 730.
26. C. Xue, Q. Han, Y. Wang, J. Wu, T. Wen, R. Wang, J. Hong, X. Zhou and H. Jiang, *Biosens. Bioelectron.* , 2013, **49**, 199.
27. M. Liu, Q. Chen, C. Lai, Y. Zhang, J. Deng, H. Li and S. Yao, *Biosens.*

Bioelectron., 2013, **48**, 75.
28. X. Kan, Y. Zhao, Z. Geng, Z. Wang and J.-J. Zhu, *J. Phys. Chem. C*, 2008, **112**, 4849.
29. X. Dong, Y. Ma, G. Zhu, Y. Huang, J. Wang, M. B. Chan-Park, L. Wang, W. Huang and P. Chen, *J. Mater. Chem.* , 2012, **22**, 17044.
30. G. Zhu, Z. He, J. Chen, J. Zhao, X. Feng, Y. Ma, Q. Fan, L. Wang and W. Huang, *Nanoscale*, 2014, **6**, 1079.
31. A. Reina, X. Jia, J. Ho, D. Nezich, H. Son, V. Bulovic, M. S. Dresselhaus and J. Kong, *Nano Lett.* , 2009, **9**, 30.
32. Z. Guo, S. Wang, G. Wang, Z. Niu, J. Yang and W. Wu, *Carbon*, 2014, **76**, 203.
33. H. R. Thomas, C. Valles, R. J. Young, I. A. Kinloch, N. R. Wilson and J. P. Rourke, *J. Mater. Chem. C*, 2013, **1**, 338.
34. J. P. Rourke, P. A. Pandey, J. J. Moore, M. Bates, I. A. Kinloch, R. J. Young and N. R. Wilson, *Angew. Chem.Int. Edit.*, 2011, **50**, 3173.
35. Z. Chen, D. Higgins, H. Tao, R. S. Hsu and Z. Chen, *J. Phys. Chem. C*, 2009, **113**, 21008.
36. H. C. Choi, S. Y. Bae, W. S. Jang, J. Park, H. J. Song, H. J. Shin, H. Jung and J. P. Ahn, *J. Phys. Chem. B*, 2005, **109**, 1683.
37. X. Feng, Y. Zhang, Z. Yan, N. Chen, Y. Ma, X. Liu, X. Yang and W. Hou, *J. Mater. Chem. A*, 2013, **1**, 9775.
38. S. J. Tian, A. Baba, J. Y. Liu, Z. H. Wang, W. Knoll, M. K. Park and R. Advincula, *Adv. Funct. Mater.*, 2003, **13**, 473.
39. X. Dong, X. Wang, L. Wang, H. Song, H. Zhang, W. Huang and P. Chen, *ACS Appl. Mat. Interfaces*, 2012, **4**, 3129.
40. L. Liu, J. Du, S. Li, B. Yuan, H. Han, M. Jing and N. Xia, *Biosens. Bioelectron.* , 2013, **41**, 730.
41. J. Liu, Z. He, J. Xue and T. T. Y. Tan, *J. Mater. Chem. C*, 2014, **2**, 2478.
42. S. Hou, M. L. Kasner, S. Su, K. Patel and R. Cuellari, *J. Phys. Chem. C*, 2010, **114**, 14915.
43. C.-L. Sun, C.-T. Chang, H.-H. Lee, J. Zhou, J. Wang, T.-K. Sham and W.-F. Pong, *ACS Nano*, 2011, **5**, 7788.
44. G. T. S. How, A. Pandikumar, H. N. Ming and L. H. Ngee, *Sci. Rep.*, 2014, **4**, 5044.
45. Y. J. Shin, Y. Wang, H. Huang, G. Kalon, A. T. S. Wee, Z. Shen, C. S. Bhatia and H. Yang, *Langmuir*, 2010, **26**, 3798.